Orientational selectivity is retained in zero-crossings obtained via stochastic resonance

Ajanta Kundu[1], Sandip Sarkar[2]

[1]Applied Nuclear Physics Division, Saha Institute of Nuclear Physics, 1/AF Bidhannagar, Kolkata-700064, India.

[2]Applied Nuclear Physics Division, Saha Institute of Nuclear Physics, 1/AF Bidhannagar, Kolkata-700064, India.

{[1]ajanta.kundu@saha.ac.in; [2]sandip.sarkar@saha.ac.in }

Abstract: Computational theory of visual information processing suggest that the initial stages information processing consists of in part representation of zero crossing in the visual scene filtered through a suitable second order differential operator (centre-surround receptive field). These zero crossings often correspond to sharp intensity changes in the visual scene and are rich in information. We report here our investigation, through simulation study, on the role of zero crossings in orientational selectivity measurement. We show that the perceptive contrast sensitivity of zero-crossing of sub-threshold noise contaminated grating image exhibit stochastic resonance. We also show that the contrast sensitivity of test grating, in the presence of a masking grating, decreases with the increase of masking contrast.The qualitative nature of the contrast sensitivity variations are in agreement with the results of various phychophysical experiments.

Keywords: zero-crossing, contrast sensitivity, stochastic resonance, receptive field, LoG

1 Introduction

It has been demonstrated in many experiments that the addition of external noise to a weak signal can enhance its detectability by the peripheral nervous system of crayfish [1], cricket [2] and also human [3-7]. Direct evidences of performance enhancement for noise contaminated visual inputs have been demonstrated through psychophysical experiments [5-8]. It has been shown [7, 8] that the brain is capable of extracting detail in a stationary image masked with noise. The perceived image quality is strongly dependent on noise intensity. It has been observed that the detection of sub-threshold images, mediated by threshold crossing[1] (different from zero-crossing) events in the presence of noise improves non-

J. C. Bansal et al. (eds.), *Proceedings of Seventh International Conference on Bio-Inspired Computing: Theories and Applications (BIC-TA 2012),* Advances in Intelligent Systems and Computing 202, DOI: 10.1007/978-81-322-1041-2_17,

monotonically with noise power. For all the experiments involving visual input the retinal computational network does the basic information processing which can be explained by center-surround receptive field [9, 10], Computational theory of visual information processing suggest [10-12] that the information processing, in the initial stages, consists of in part representation of zero crossings in the visual scene filtered through a suitable second order differential operator (usually $\nabla^2 G$ of different sizes where G is Gaussian). The prime motivation behind this suggestion is that the zero crossings often correspond to sharp intensity changes in the visual scene usually referred to as edges. These edges often correspond to surface discontinuities or surface reflectance or illumination boundaries of the visual environment. It has been also observed in speech experiment [13] that with only the zero-crossing information much of the information content of the speech could be retained. Studies in visual information processing [11, 14] also stresses the importance of the information content of zero-crossings in classifying visual scene.

Zero crossings (ZC) are, therefore, play an important role in the information retrieval but very little is known about its role in visual information processing that leads to noise induced performance enhancement. We investigate here the role of ZCs of sub-threshold image filtered through centre-surround receptive field in perceptive contrast sensitivity (PCS) enhancement in the presence of noise. We show that the PCS of ZC image is strongly dependent on the external noise strength and PCS attains a maximum for an optimal amount of noise via stochastic resonance (SR). We also show that the contrast sensitivity of ZCs test grating, in the presence of a masking grating, decreases in direct proportion to the masking contrast. Some important observations are that the qualitative nature of the contrast sensitivity variations is in agreement with the results of psychophysical experiment [7, 15].

2 Theoretical considerations

The very first stage of vision involves detection of intensity changes or ZC of the visual scene for the formation of the "raw primal sketch" [9, 10, 16, 17]. It is, therefore, expected that the ZC has a considerable role in visual information processing that leads to noise induced performance enhancement via a phenomenon called SR [18]. In natural image intensity changes occur over wide range of scales. At any given scale it can be detected, for an image I(x,y), by finding zero values of $\nabla^2 G(x,y;t) \otimes I(x,y)$ where $G(x,y;t)$ is Gaussian function in two dimension with variance t, ∇^2 is the Laplacian and $\otimes$ represent convolution. For our analysis we revisit the proposition of Ernst Mach [19, 20] which states that the brightness sensation at any retinal point is the combined effect of the original illumination and its second differential quotient. The corresponding spatial filter function for a given scale t can then be written as

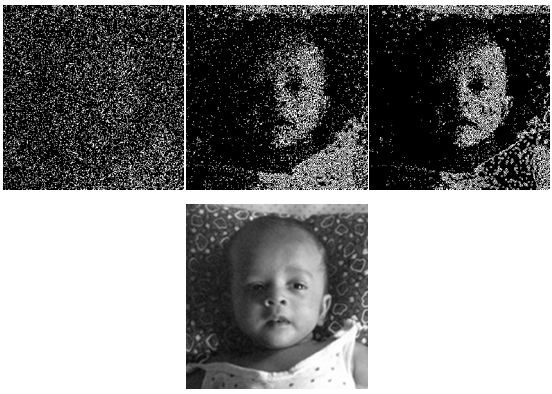

Fig. 1 This is a visual illustration of ZC, in the presence of additive noise, of a natural image *S* (infant portrait in the bottom row) digitized on a 0 to 1 gray scale. First the image *S* is pushed below threshold (defined by gray value 0), such that its mean lies Δ below the threshold resulting in the image $S - \Delta - \mu_S$ where the mean intensity of S is μ_S. After adding a random number ξ, from a zero-mean Gaussian distribution with standard deviation σ_n, to the original gray value S of every pixel, the image is convolved with filter mask (Equation (1)) resulting in $(S - \Delta - \mu_S + \xi) \otimes h(x, y; t)$. ZCs are then detected according to the following rule: if $sgn((S - \Delta - \mu_S + \xi) \otimes h(x, y; t))$ of any two consecutive pixels, either in the horizontal or in the vertical direction, is opposite, the gray value of the pixel with negative sign is made 0 (black), and the gray value of the other one is made 1 (white). For all other pixels the gray value is replaced with 0 (black). Three such cases are shown for $\sqrt{t} = 2.1, \sigma_0 = -0.15$, $m = 0.2$, $\sigma_n = 0.18$ and for contrast=0.1, 0.6 and 0.9 from left to right in the upper row.

$$h(x, y; t) = \delta(x, y) - m\nabla^2 G(x, y; t) \tag{1}$$

Where $\delta(x, y)$ is Kronecker delta function, m is a constant factor, and $G(x, y; t)$ is the Gaussian defined by

$$G(x, y; t) = \frac{1}{2\pi t} e^{\frac{-(x^2+y^2)}{2t}} \tag{2}$$

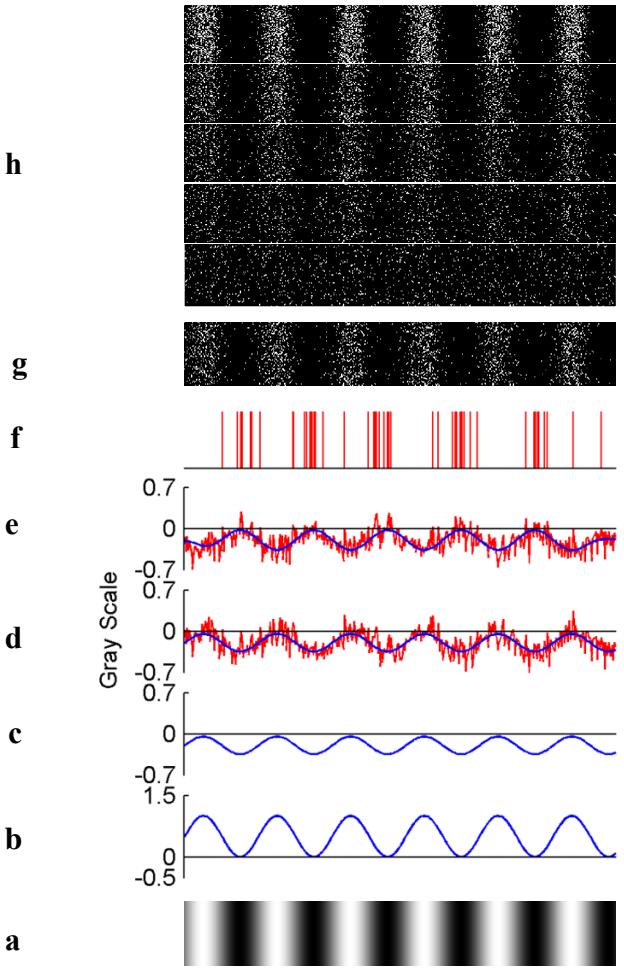

Fig. 2 (a) The sinusoidal grating image I with a spatial resolution of 512 by 512 pixels used for our experiment was generated by the spatial function $0.5A\sin(2\pi fx)+0.5$, where A is Michelson contrast[3], f is the spatial frequency in cycles/pixel and x is the horizontal coordinate in pixel. For the sake of illustration the image, with reduced spatial resolution of 400 by 64 pixels, is displayed with maximum contrast A=1. (b) The intensity variation along horizontal directions shown here. (c) After setting A=0.3, image is then pushed below the threshold (gray value 0), as depicted by the intensity profile in the figure, such that its mean lies $\Delta = 0.25$ below the threshold resulting in the image $I-(0.5+\Delta)$. (d) This is the resultant profile obtained after the addition of Gaussian noise of appropriate amount to the sub-threshold image, (e) The noise contaminated image is then convolved with the filer function $h(x,y;t)$. The resultant effect is visually represented in this figure. And in (f) the corresponding ZCs are depicted by a vertical line of equal height. (g) The resultant ZC image is shown where black dots (gray value of 0) represent ZC and the white dots (gray value of 1) represent absence of ZC. And in (h) similar ZC images with A= 0.05, 0.1, 0.2 0.3, 0.5 are shown.

and t is its variance. This kind of representation is well suited for linear scale space theory of early visual operations [21-23]. This theory shows that Gaussian and its derivatives form a complete set of operators for multi-scale representation of an image. Additionally this computational paradigm is also in agreement with the biological visual computation. Studies [24, 25] have shown that superposition of Gaussian and its derivatives can be used to model the receptive field profiles of mammalian retina and visual cortex. Our focus is to study the behavior of ZC (filtered through $h(x, y; t)$) of sub-threshold images with additive noise contamination in contrast sensitivity measurement.

3 Methods

The necessary components are a filter function that mimics image enhancement in retina, a threshold (gray value 0), a threshold crossing detector, an image and an additive Gaussian noise. For demonstration a natural image of a face $S(x, y)$, as shown in Figure 1, and a sampled version[2] of the continuous filter function (Equation (1)), is used for the experiment. ZCs computed from the filtered images and the resultant output images for three cases with increasing contrast (left to right)are displayed. Though these are basically binary images containing pixels whose gray values are either 1 or 0, we could still perceive shading effect because the original intensity variation is mapped to ZC density variation through the process of ZC image formation thereby producing halftone like effect. Visually the first image, which is of lower contrast, is devoid of all shadow details. The third image, with much higher contrast, could retain comparatively better shadow details of the original face image. The middle ZC image, with intermediate contrast, on the other hand could retain best shadow detail. This simple experiment illustrates that the best representation of the original image can be achieved for an intermediate contrast level for a given amount of additive Gaussian noise contamination. We will study this phenomenon in more detail in all our experiments described below. In all the experiments, we have expressed the frequency f in cycles/pixel to avoid the explicit dependence of the visual angle. This can be converted to cycles/degree by the multiplication of an appropriate constant K_v , in pixel/degree, which is a function of the angle the image subtends at the viewer's eye.

4 Experiment 1

For a quantitative study, we choose a sinusoidal grating image generated by a function as shown in Figure 2(a) where a full contrast noise free grating image, without threshold filtering, is displayed. Its intensity variation along horizontal direction is shown in Figure 2(b).The resulting image profile, after contrast modification followed by threshold filtering by an amount Δ , will look like as shown in Figure 2(c). After the addition of a zero mean Gaussian noise a typical image profile will look like as shown in Fig. 2(d). This noise contaminated image is then

convolved with the filter function given by Equation (1) resulting in the image determined by $(I-\Delta-0.5+\xi)\otimes h(x,y;t)$. A typical profile of this image is shown in Figure 2(e). Clearly, noise of appropriate amount helps in mediating threshold (gray value of 0) crossing events. These zero crossings (ZCs) are represented by a vertical line of unit length as depicted in Figure 2(f).The final ZC image, a binary image consisting of gray value 0 and 1, is illustrated in Figure 2(g). Here black dots (gray value of 0) represent ZC and the white dots (gray value of 1) represent absence of ZC. Starting from the grayscale pattern (Figure 2(a)) we arrive at the binary image, as in Figure 2(f), where only one bit of information marking ZC events, computed by our experimental system as described in Figure 2, is retained in every pixel. Varying only the contrast the whole process is repeated to compute the corresponding ZC image. Five such images are shown in Figure 2(h), with in-

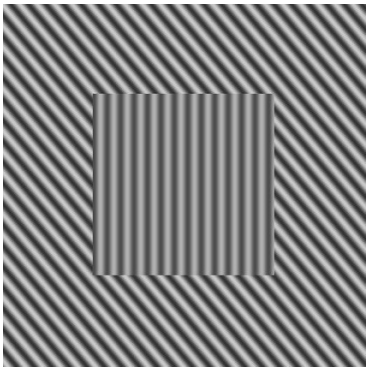

Fig. 3 Typical image that is used for studying the contrast sensitivity variation in the presence of a mask is displayed. The background is the mask of spatial resolution 512x512 and the test grating is placed at the center of the mask. The sinusoidal grating image,with a spatial resolution of 256 by 256 pixels,is generated by the spatial function $0.5A\sin(2\pi fx)+0.5$, where A is Michelson contrast[3], $f$is the spatial frequency in cycles/pixel and x is the horizontal coordinate in pixel. The background is an oriented sinusoidal grating with frequency equal to that of the test grating at the center.

creasing (bottom to top) contrast values. Visual inspection reveal that for low contrast the image looks devoid of any features and as the contrast is increased, the grating specific features begin to appear. With further increase in contrast, the images begin to look like square grating (loss of contrast detail). We can, therefore, visually identify an intermediate contrast for which the ZC images attain closest resemblance with the original sinusoidal grating. We mark this contrast as A_{opt} (optimal one) for the given noise. Numerically this is performed by inspecting the ZC images in the Fourier domain and looking for the maximum contrast for which the second harmonic does not appear. Similarly, by varying the noise

strength and repeating the whole process we can identify an optimal contrast value for each of the noise strengths.

5 Experiment 2

This experiment is designed as follows. A test sinusoidal grating of resolution 256x256 pixels is placed at the center of a mask of resolution 512x512 pixels (Fig. 3). The mask is composed of another grating of the same spatial frequency but

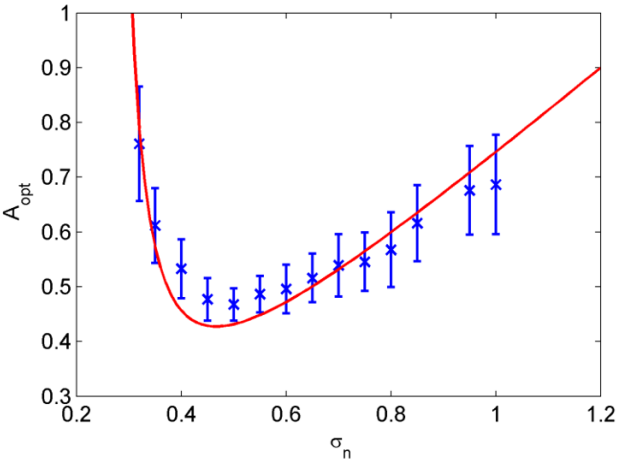

Fig. 4 Plots of optimal contrast A_{opt} versus the noise strengths σ_n for $\sqrt{t} = 2.1268$ and frequency $f = 0.10547$ cycles/pixelis shown. Each of the contrast value was computed for twenty times for twenty noise intensities. The error bars are the standard deviations of twenty A_{opt} values at each of the noise strength. The variation of optimal contrast as a function of noise strength is shown for $m = 2$, $\Delta = 0.3164$, $K = 0.8193$ and $\sigma_0 = -0.15$. The solid curve (red) is given by Equation (3) where the parameters *K* and σ_0 are obtained from nonlinear least square fit to the data (in blue) obtained in the experiment described in Fig 2.

oriented at angle with the test grating. By performing the experiment 1 with this image, as shown in Fig. 3, we will get an optimal contrast value for the test grating. When the experiment 1 is repeated by varying the contrast for a fixed orientation angle of the masking grating, we will get the variation of contrast sensitivity of the test grating as a function of the masking contrast. Again by repeating the experiment for different orientation angels, contrast variation for different orientation is obtained.

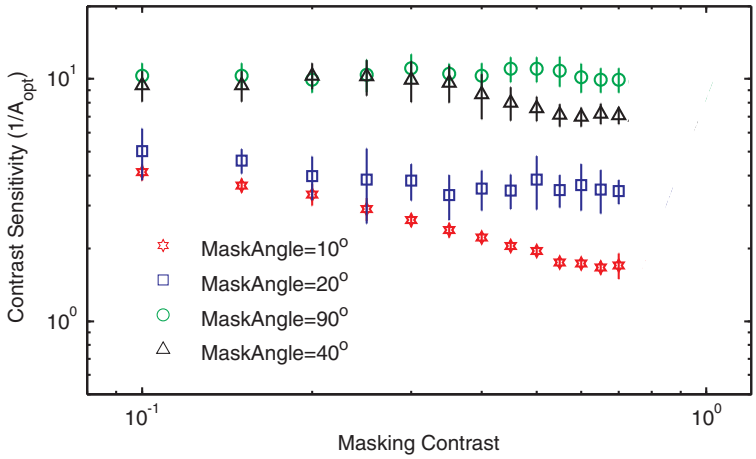

Fig. 5 Contrast sensitivity ($1/A_{opt}$) of test gratings, as shown in Fig. 3, are plotted as a function of the masking contrasts at different orientation angels: 10°, 20°, 40° and 90°. For the whole experiment $\sqrt{t} = 4.2536$ and frequency of the test grating is kept at $f = 0.0527$ cycles/pixel. Each of the contrast value is computed for ten times.

6 Results and discussion

The results of the study described in Fig. 2 and Fig. 3 are presented in Fig. 4 and Fig. 5. Results of Experiment 1 are summarised in Fig. 4 where the variation of A_{opt} with noise strength is plotted. The solid curve (red) given by

$$A_{opt} = K(\sigma_n + \sigma_0)\exp(\Delta^2 / 2(\sigma_n + \sigma_0)^2 \tag{3}$$

is the power spectrum of a pulse train, as shown in Fig. 2(e) and Fig. 3(g), and is taken from the threshold SR theory [7, 26]. The left hand side is the signal amplitude and *K* on the right hand side is proportional to signal power density. We have introduced an additional fitting parameter σ_0 in equation (3). The equation is fit to the data (blue) using *K* and σ_0 as the adjustable parameters. The quality of the fit to the simulated data is very encouraging. The good quality of the fit reveals that optimal contrast is proportional to the power contained in the signal (image) and therefore *K* can be regarded as a quantitative measure of the sensitivity to the power contained in the signal. *K* can also be regarded as a quantitative measure of the ability to distinguish details in images in the presence of additive Gaussian noise because A_{opt} in equation (3) is the optimal contrast value necessary for matching a ZC image with its original counterpart (as described in Fig. 2). Important findings are the following. (a) From the distribution of the data points in Fig. 4 it is evident that the optimal contrast varies non-monotonically with noise power and attains a minimum for an intermediate noise power which is a typical signature of SR. (b) The good quality fit of equation (3) (solid red curve) in Fig. 4 implies that the optimal contrast is proportional to the power contained in the image

which is in line with the results obtained in [7]. (c) The fitted K value can be regarded as a quantitative measure of the ability to distinguish fine details in a sub-threshold visual scene in the presence of additive Gaussian noise.
In Fig. 5contrast sensitivity of the test grating is plotted as a function of masking contrast at different orientation angles. For each of orientations angles, we get optimal contrast values, obtained via stochastic resonance, as a function of masking contrast. Inverse of measured contrast values, which is contrast sensitivity, are plotted in Fig. 5 as a function of masking contrast. It is evident from the figure that the contrast sensitivity decreases with the increase in the masking contrast. Our observation also shows that the masking effect is the maximum for the lowest orientation angle and the effect decreases with the increase of the angle. An important point to note is that the qualitative nature of these variations produced with the help of zero-crossings only, is also in agreement with the psychophysical studies [15].

7 Conclusions

Results of Experiment 1 & 2 show that the optimal contrast (contrast threshold) of images, formed from ZCs points alone, varies non-monotonically with noise power and attains a minimum, which signifies maximum contrast sensitivity, for an intermediate noise power, which is a typical signature of SR. These results are in agreement with the results of psychophysical experiments, which are evident from the goodness of fit of equation (3) to the simulated data. In other words, information content of ZCs alone can demonstrate the qualitative features of a subject's ability to distinguish fine details in noisy sub-threshold scenes via stochastic resonance. Our study also show that the measured (simulated) contrast sensitivity decreases with the increase of masking contrast and the masking effect decreases with the increase of masking angle. This behavior is qualitatively similar to the one observed in psychophysical studies [15]. An important point to note is that equation (3), which is fit to our simulated data obtained from ZCs points, is derived from the Fourier Transform of identical pulse trains similar to the neuron action potentials [26-28]. This essentially indicates that human brain may make use of similar ZC computation while processing noisy sub-threshold images. Though we do not advocate that ZCs can explain everything but all these results may provide some clues to ZC computation in our brain. These results are, therefore, may also be useful to study and analyze visual information processing.

Footnotes

[1]In case of threshold crossing all the events for which a function crosses a threshold is considered. On the contrary, for zero-crossing, only those events for which the function changes sign are considered.

[2]Use of sampled kernel can lead to implementation problems because the discrete version may not have the discrete analogs of the properties of the continuous function. For Gaussian function $G(n,t)$, truncated to give finite

impulse response, the support is generally chosen large enough such that $2\int_{u=M}^{\infty} G(u,t)du < \epsilon$. A common choice of M is $M = C\sqrt{t}+1$, where C is constant. For small values of ϵ ($\leq 10^{-6}$) the errors introduced by truncating the Gaussian are usually negligible. For our study $\varepsilon \leq 10^{-10}$ ($\sqrt{t}$ =2.12 and C $\geq$ 6).

[3]If I_{min} and $I_{\max}$ are the minimum and maximum intensity respectively in an image then the Michelson contrast is defined as $(I_{max} - I_{min}) / (I_{max} + I_{min})$

References

[1] Douglass, J. K., Wilkens, L., Pantazelou, E., Moss, F.: Noise enhancement of information transfer in crayfish mechanoreceptors by stochastic resonance, Nature, 365,337-340 (1993).

[2] Levin, J. E., Miller, J. P.: Broadband neural encoding in the cricket cercal sensory system enhanced by stochastic resonance, Nature, 380, 165-168 (1996).

[3] Chiou-Tan, F.Y., Magee, K.N., Robinson, L.R., Nelson, M.R., Tuel, S.S., Krouskop, T.A., Moss, F.: Enhancement of Subthreshold Sensory Nerve Action Potentials During Muscle Tension Mediated Noise. Intern. J. Bifurc. Chaos, 7, 1389. (1996).

[4] Collins, J. J., Imhoff, T. T., Grigg, P.: Noise-enhanced tactile sensation. Nature, 383, 770. (1996).

[5] Kitajo, K., Nozaki, D., Ward, L.M., Yamamoto, Y.: Behavioral Stochastic Resonance within the Human Brain. Phys.Rev. Lett. 90, 218103 (2003).

[6] Mori, T., Kai, S.: Noise-Induced Entrainment and Stochastic Resonance in Human Brain Waves, Phys. Rev. Lett. 88, 218101 (2002).

[7] Simonotto, E., Riani, M., Seife, C., Roberts, M., Twitty, J., Moss, F.: Visual Perception of Stochastic Resonance. Phys. Rev. Lett. 78, 1186-1189 (1997).

[8] Goris, R. L. T., Zaenen, P., Wagemans, J.: Some observations on contrast detection in noise. Journal of Vision 8(9):4, 1-15 (2008).

[9] Marr, D.: Vision: A Computational Investigation into the Human Representation and Processing of Visual Information. W H Freeman and Company, New York (1982).

[10] Marr, D., Hildreth, E.: Theory of Edge Detection. Proc. R. Soc. Lond. Series B, Biological Sciences. 207. 187-217 (1980).

[11] Marr, D., Ullman, S., Poggio, T.: Bandpass channels, Zero crossings, and early visual Information processing. J. Opt. Soc. Am., 69(6), 914-916 (1979).

[12] Marr, D., Ullman, S.: Directional selectivity and its use in early visual processing. Proc. Soc. Lond. B 211, 151-180 (1981).
[13] Licklider, J. C. R., Pollack, I.: Effects of differentiation, integration and infinite peak clipping upon the intelligibility of speech. J. Acoust. Soc. Amer., 20, 42-51 (1948).
[14] Curtis, S. R., Oppenheim, A. V., Lim, J. S.: Reconstruction of two-dimensional signals from threshold crossings. Acoustics, Speech, and Signal Processing, IEEE International Conference on ICASSP '85, 10, 1057 – 1060 (1985).
[15] Campbell, F. W. and Kulikowski, J. J. : Orientational selectivity of the human visual system. J. Physiol. (1966), 187, 437-445 (1966).
[16] Marr, D., Poggio, T., Ullman, S. J.: Opt. Soc. Am. 70: 868-70 (1979).
[17] Ullman, S.: Artificial Intelligence and The Brain: Computational Studies of the Visual System. Ann. Rev. Neuroscience, 9, 1-26 (1986).
[18] Sarkar, S., Ghosh, K., Bhaumik, K.: Proceedings of the 3rd Indian International Conference on Artificial Intelligence, Pune, India, December (2007), ISBN 978-0-9727412-2-4.
[19] Mach, E. (1868). On the physiological effects of spatially distributed light stimuli. Translated in F Ratliff, "Mach Bands: Quantitative Studies on Neural Networks in the Retina," Holden-Day, Sanfrancisco, 299-306, (1965).
[20] Mead, C.: Neuromorphic electronic systems. Proceedings of the IEEE, 78(10), 1639-1636 (1990).
[21] Koenderink, J. J. : The Structure of Images. Biological Cybernetics, 50, 363–370 (1984).
[22] Lindeberg, T. : Scale-Space Theory: A Basic Tool for Analyzing Structures at Different Scales. Journal of Applied Statistics 21 (2), 224–270 (1994).
[23] Yuille, A. L., and Poggio, T.A.: Scaling Theorems for Zero Crossings. IEEE Trans. Pattern Analysis & Machine Intelligence, PAMI-8(1), 15–25 (1986).
[24] Young, R. A.: The Gaussian derivative model for spatial vision: I. Retinal mechanisms. Spatial Vision2 (4), 273–293 (1987).
[25] Young, R. A., Lesperance, R. M., and Meyer, W. W.: The Gaussian Derivative model for spatial-temporal vision: I. Cortical model. Spatial Vision 14 (3-4), 261–319 (2001).
[26] Gingl, Z., Kiss, L. B., Moss, F.: Non-Dynamical Stochastic Resonance: Theory and Experiments with White and Arbitrarily Colored Noise. Europhys.Lett.29 (3), 191-196 (1995).
[27] Gingl, Z., Kiss, L., Moss, F.: Nuovo Cimento D, 17, 795 (1995).
[28] Campbell, F. W., Robson, J. G.: Application of Fourier analysis to the visibility of grating, J. Physiol. 197, 551-566 (1968).